RAA 2016 Vol. **16** No. **1**, 8 (6pp) doi: 10.1088/1674–4527/16/1/008
http://www.raa-journal.org *http://iopscience.iop.org/raa*

***R**esearch in*
***A**stronomy and*
***A**strophysics*

Study of temporal evolution of emission spectrum in a steeply rising submillimeter burst

Jian-Ping Li[1,2], Ai-Hua Zhou[1,2] and Xin-Dong Wang[3]

[1] Key Laboratory of Dark Matter and Space Astronomy, Chinese Academy of Sciences; Nanjing 210008, China; *zhouah@pmo.ac.cn*
[2] Purple Mountain Observatory, Chinese Academy of Sciences, Nanjing 210008, China
[3] School of Public Administration, Hohai University, Nanjing 210098, China

Received 2015 March 11; accepted 2015 June 11

Abstract The temporal evolution of a spectrum during a steeply rising submillimeter (THz) burst that occurred on 2003 November 2 was investigated in detail for the first time. Observations show that the flux density of the THz spectrum increased steeply with frequency above 200 GHz. Their average rising rates reached a value of 235 sfu GHz^{-1} (corresponding to spectral index α of 4.8) during the burst. The flux densities reached about 4 000 and 70 000 sfu at 212 and 405 GHz at the maximum phase, respectively. The emissions at 405 GHz maintained such a continuous high level that they largely exceeded the peak values of the microwave (MW) spectra during the main phase. Our studies suggest that only energetic electrons with a low-energy cutoff of $\sim$1 MeV and number density of $\sim 10^6$–10^8 cm^{-3} can produce such a strong and steeply rising THz component via gyrosynchrotron radiation based on numerical simulations of burst spectra in the case of a nonuniform magnetic field. The electron number density *N*, derived from our numerical fits to the THz temporal evolution spectra, increased substantially from 8×10^6 to 4×10^8 cm^{-3}, i.e., the *N* value increased 50 times during the rise phase. During the decay phase it decreased to 7×10^7 cm^{-3}, i.e., it decreased by about five times from the maximum phase. The total electron number decreased an order of magnitude from the maximum phase to the decay phase. Nevertheless, the variation in amplitude of *N* is only about one time in the MW emission source during this burst, and the total electron number did not decrease but increased by about 20% during the decay phase. Interestingly, we find that the THz source radius decreased by about 24% while the MW source radius, on the contrary, increased by 28% during the decay phase.

Key words: Sun: submillimeter burst — Sun: energetic electrons — Sun: radio source size

1 INTRODUCTION

The diagnostics of highly relativistic electrons and emission source regions in solar flares are essentially based on their emission spectra at various wavelength ranges (Gary 1985; Wang et al. 1994; Zhou & Karlicky 1994; Zhou et al. 2005; Huang et al. 2005; Zhou et al. 2009). The spectral maximum of the microwave (MW) emission is typically in the range of 3–30 GHz, depending primarily on the energy of the accelerated electrons. There are rare spectral examples of MW peaking at higher frequencies, up to 94 GHz for solar observations made in the past (Croom 1973; Kaufmann et al. 1985; Ramaty et al. 1994; Chertok et al. 1995). Since 2000, new instrumentation observing in the 200–400 GHz range have become available, and more than 10 flares have been observed in this band (Silva et al. 2007; Krucker et al. 2013). For some flares these observations show that the gyrosynchrotron (GS) component extends up to 200 GHz (Trottet et al. 2002) or higher frequencies (Lüthi et al. 2004b). However, for other flares the radio spectrum above 200 GHz is not a continuation of the GS spectrum measured at lower frequencies, but surprisingly increases with increasing frequency (Silva et al. 2007; Lüthi et al. 2004a; Kaufmann et al. 2004). This spectral feature is termed a "THz component."

So far, there have been various possible explanations proposed for the new increasing submillimeter spectral component, but many theoretical issues remain open (Zhou et al. 2011; Krucker et al. 2013). We think that the GS emission is a possible mechanism of the THz emission. But under the assumption of a uniform source, an extreme value of the magnetic field of 4500 G and a high electron number density of 1.7×10^{12} cm^{-3} are required in the explanation of GS emission (Silva et al. 2007). These requirements can be decreased to a reasonable range by using our GS radiation model that includes self and gyroresonance absorptions (Zhou et al. 2008) in a nonuniform magnetic field model (Zhou et al. 2011).

Thus far, spectra with a positive slope have only been observed in a handful of the most energetic events

(Krucker et al. 2013), so THz burst observations are very valuable, especially for the 2003 November 2 burst which has a set of complete observations of the temporal evolution of the spectra in THz. These observations can provide important diagnostics about the energy release process of ultrarelativistic electrons and variation of the environment in the THz burst region in deeper layers of the solar atmosphere (about 1000–30 000 km above the photosphere).

In this paper, we will investigate this set of temporal evolution spectra in detail for the first time. A vast amount of numerical simulations for these temporal evolution spectra have been done by using the GS emission model in the case of a dipole magnetic dipole. We try to obtain a diagnostic of the physical parameters of highly relativistic electrons and their environment in the solar THz and MW burst regions. Then we compare the temporal evolution results about the electron number density and source size in the MW and THz burst regions. Finally, we give a summary and conclusions.

2 OBSERVATIONS

Extensive flare activities were observed in super-AR NOAA 10486 during its disk passage (2003 October 22 - November 4). Among them, an increasing submillimeter burst was detected by the Solar Submillimeter Telescope (SST) at 212 and 405 GHz in the flare starting at ∼17:16 UT on 2003 November 2. The flare was also detected simultaneously by the Owens Valley Solar Array (OVSA) at MW wavelengths (see Fig. 1). The maximum phase, main phase, and decay phase are shown in Figure 1 according to the time profiles of the THz burst. This flare was classified as a GOES X8.3 and 2B event.

Figure 2 displays the temporal evolutions of the emission spectrum at the MW and THz wavelengths. It indicates that at 17:16:15 UT of the rise phase, the OVSA radio flux densities reached, respectively, 5.1×10^3 and 3×10^4 sfu at 3 and 18 GHz in the MW range; and $\sim 1.2 \times 10^3$ and 3.1×10^4 sfu at 212 and 405 GHz in the THz range. At the maximum phase the flux densities increased dramatically to 8×10^3 and 4×10^4 at 3 and 18 GHz respectively; and 4×10^3 and 7×10^4 sfu at 212 and 405 GHz respectively. After the maximum phase, the flux densities gradually decreased until 17:18:00 UT. In a period of 17:18:00 to 17:18:30 UT the flux densities of the submillimeter spectrum increased once again, but this increase of flux density did not occur in the MW range, which means that more energetic electrons were accelerated to higher energies in that period. After ∼17:20:30 UT the MW and THz emissions decreased further. The flux densities at 405 GHz were so high that they exceeded the peak flux densities of the MW spectrum during the main phase.

3 INCREASING RATE OF FLUX DENSITY OF SUBMILLIMETER BURST SPECTRUM

It is found from Figure 2 that the rising rate of the flux density, *r* (sfu GHz^{-1}), changes greatly in the THz spectrum range during the burst. The rising rate obtained from the observational spectra increased from 154 to 342 sfu GHz^{-1} during the rise phase (see Table 1). During the decay phase, it decreased from 342 to 142 sfu GHz^{-1}, i.e., the rising rate at the maximum phase is much higher than that at the rise phase or decay phase. The average value of *r* reached 235 sfu GHz^{-1} (corresponding to a spectral index α of 4.8 at the optically thick part) during this flare. Thus, it is a steeply rising THz burst.

4 FIT FOR THE STEEPLY RISING SUBMILLIMETER BURST SPECTRUM

It is well known that the radio spectrum can provide crucial information about energetic electrons and their environment in solar flares. This information mainly contains the energy spectral index δ, low- and high-energy cutoffs E_0 and E_m respectively, electron number density *N*, source radius R, and magnetic field strength B in source regions. The magnetic field strength B can be estimated in the case of a dipole magnetic field if the photospheric magnetic field strength B_0, the lower boundary height of THz source h_{d}, and the corresponding upper one h_{u} can be determined (Zhou et al. 2008, 2011). A set of reasonable values of the parameters is taken as $\delta = 3$, B_0 = 5000 G, $R = 0.5''$, h_{d} = 10^8 cm, and $h_{\mathrm{u}} = 3 \times 10^9$ cm for the THz spectra based on our numerical simulations; so only the energy cutoffs E_0 and E_m, and electron number density *N* remain unknown.

Figure 3 shows that the effect of increasing the high-energy cutoff E_m on the THz spectrum only enhances the GS emission at the optically thin part a little and at the optically thick part it is constant. Hence, the E_m value of 10 MeV is high enough for calculations of the THz burst spectrum. Finally, the remaining unknown parameters are only E_0 and *N*. In the paper we try to derive the two parameters from the fits to observations of the spectral evolution in THz.

Figure 2 shows that their flux densities reached about 4000 and 70 000 sfu at 212 and 405 GHz at the maximum phase, respectively. During the main phase, the emissions at 405 GHz maintained such a continuous high level that they largely exceeded the peak values of the MW spectra. It is important to know what conditions are needed to produce such steeply rising and giant submillimeter emission.

Table 2 gives the theoretical rising rate r_{theo} sfu GHz^{-1} of the modeled submillimeter components for different number densities *N* setting $E_0 = 1$ MeV, and different low-energy cutoffs E_0 setting $N = 8 \times 10^{11}$ cm^{-3}. It shows that the theoretical rising rate r_{theo} obviously increases with increasing number density and increasing low-energy cutoff. The effects of low-energy cutoff and electron number density on the THz spectrum are given in Figure 4. It demonstrates that the THz spectral distributions are sensitive to the two parameters. We find that only the electrons with a low-energy cutoff of ∼1 MeV and number density of $\sim 10^6$–10^8 cm^{-3} can produce such steeply rising THz spectral components as the 2003 November 2 burst. Even in this case of 1 MeV

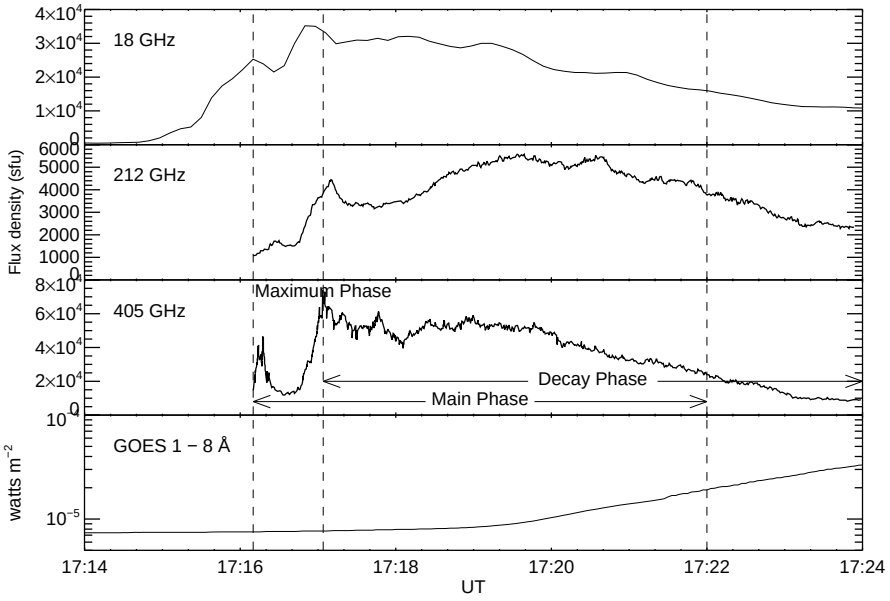

Fig. 1 Temporal evolution of the emission at 18 GHz from OVSA, 212 and 405 GHz from SST, and GOES X-ray flux of the 2003 November 2 flare. The rise phase (∼17:16 – ∼ 17:17 UT), the maximum phase (∼17:17 UT), the decay phase (∼17:17 – ∼17:24 UT, and the main phase (∼17:16 –17:22 UT) are shown in panel three.

Table 1 Rising Rates *r* sfu GHz^{-1} of the Flux Density S_ν of the THz Component During the November 2 THz Burst

Date	Time	Rise-phase	Max.-phase	Decay-phase	$S_{212\,\mathrm{GHz}}$ ($\times 10^3$)	$S_{405\,\mathrm{GHz}}$ ($\times 10^4$)	r (sfu GHz^{-1})
2003 11 02	17:16:15	yes			1.2	3.1	154
	17:17:06		yes		4.0	7.0	342
	17:17:30			yes	3.2	5.0	242
	17:18:00			yes	3.5	4.0	210
	17:18:30			yes	4.0	5.8	280
	17:19:00			yes	5.0	5.5	259
	17:19:30			yes	5.0	5.5	259
	17:20:00			yes	5.0	4.8	223
	17:21:00			yes	4.5	3.2	142

Table 2 Theoretical Increasing Rates r_{theo} sfu GHz^{-1} of the Submillimeter Spectral Components for Different Number Densities N Setting $E_0 = 1$ MeV, and for Different Low-Energy Cutoffs E_0 Setting $N = 8 \times 10^{11}$ cm^{-3}, where $\delta = 3$, $B_0 = 5000$ G, $\theta = 60^\circ$ and $h_{\mathrm{d}} = 10^8$ cm.

N (cm^{-3})	4×10^7	10^8	5×10^8	10^9
r_{theo}	64	95	180	226
E_0 (keV)	50	100	300	1000
r_{theo}	16	36	96	234

low-energy cutoff and 8×10^{11} cm^{-3} electron number density, the maximum theoretical rising rate r_{theo} only reaches 234 sfu GHz^{-1} (see Table 2), which is still smaller than the observational one (342 sfu GHz^{-1}) at the maximum phase of this THz burst.

It is also seen from Figure 4 that the maximum frequency in the THz range can reach as high as ∼2000 GHz and the GS emissions can extend to higher (>5000 GHz) frequencies in the case of 1 MeV low-energy cutoff and 8×10^{11} cm^{-3} electron number density.

Now we will try to fit the temporal evolution spectra of the THz burst for $\delta = 3$, $E_0 = 1$ MeV and source radius $R = 0.5''$. A sequence of number densities is selected to fit these spectra. The modeled GS emission spectra are given in Figure 2 by the solid lines, which indicate that the modeled spectra fit the observational ones well. The required electron number densities are given in Table 3 for the THz spectra. It demonstrates that the number density *N* increased substantially from 8×10^6 cm^{-3} at the rise phase to 4×10^8 cm^{-3} at the maximum phase in the THz

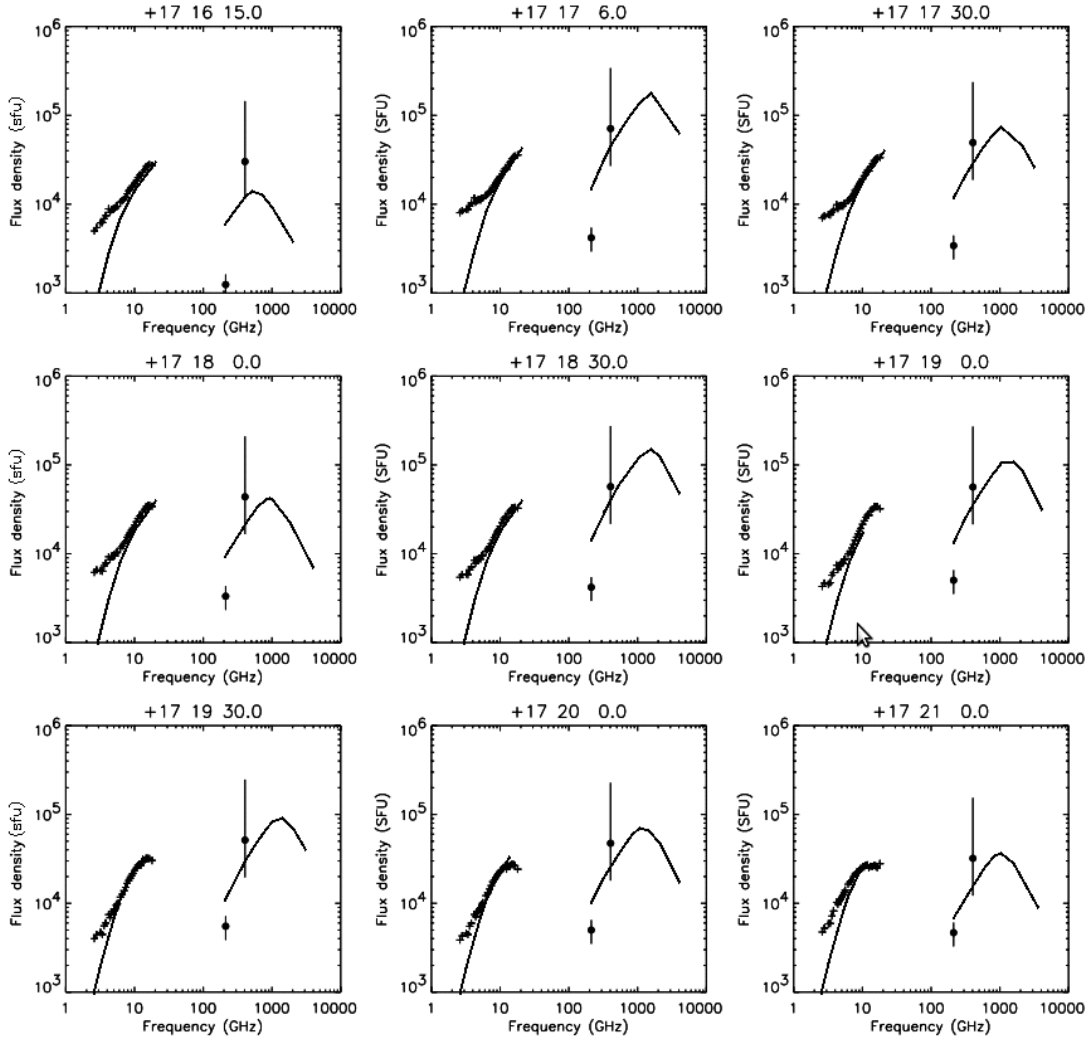

Fig. 2 The temporal evolutions of the radio spectrum from 17:16:15 to 17:21:00 UT of the 2003 November 2 burst given by Silva et al. (2007) and their fits (see *the solid lines*).

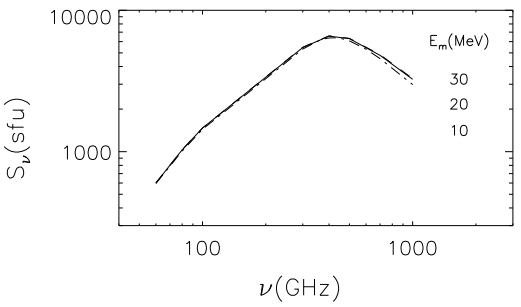

Fig. 3 Calculated GS emission spectra in the THz range in the case of a dipole magnetic field for a sequence of high-energy cutoffs E_m, where $\delta = 3$, $E_0 = 500$ keV, $N = 10^7$ cm^{-3}, $\theta = 60^\circ$, and $B_0 = 5000$ G.

source, i.e., *N* increased about 50 times. Then the electron number *N* began to drop from its maximum value, but it increased once again at 17:18:30 UT and the peak frequency of the modeled spectrum can shift to a higher frequency of 1500 GHz at that time (see Fig. 2). At 17:21:00 UT of the decay phase, the value of *N* decreased to 7×10^7 cm^{-3}, i.e., it decreased nearly five times from the maximum value. The total electron numbers $N_{\rm total}$ are also calculated in radio sources (see Table 3). We can see from Table 3 that the value of $N_{\rm total}$ in the THz source increased rapidly from 10^{31} at the rise phase to 5.2×10^{32} at the maximum phase, i.e., also increasing 50 times with the electron number density due to constant source size in that period. During the decay phase the $N_{\rm total}$ value decreased from 5.2×10^{32} to 5.3×10^{31}, i.e., it decreased about an order of magnitude.

We also define a sequence of electron number densities to fit the observational MW spectra in the case of $E_0 = 10$ keV, and $R = 25''$. We found that these modeled spectra also fit the observational spectra well from the rise phase to decay phase. The required electron number density *N* in the MW source is also given in Table 3, which shows that the value of *N* in the MW emission source increased by only about one time during the rise phase and

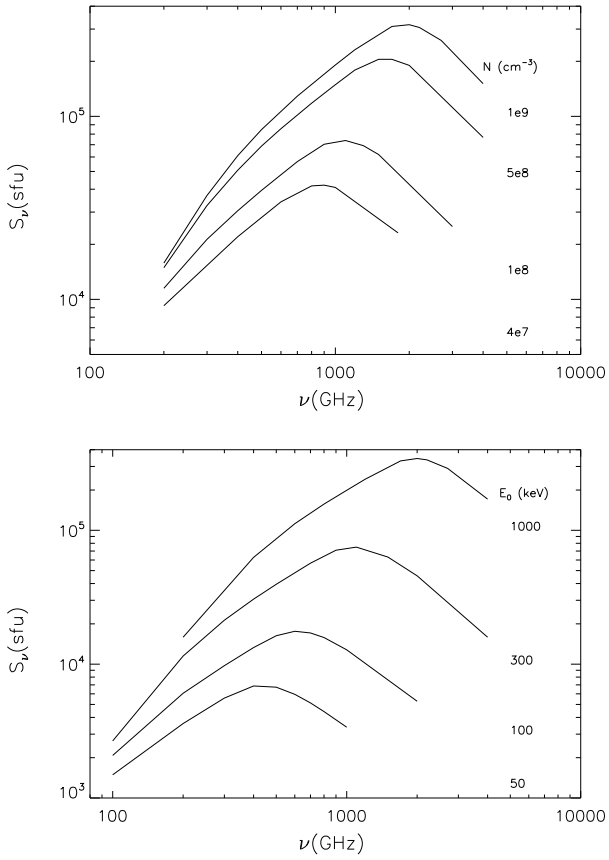

Fig. 4 Calculated GS emission spectra in the THz range in the case of a dipole magnetic field for a sequence of low-energy cutoffs E_0 setting $N = 8 \times 10^{11}$ cm^{-3} (*top panel*) and for a sequence of electron number densities *N* setting $E_0 = 500$ keV (*bottom panel*), where $\delta = 3$, $B_0 = 5000$ G, $\theta = 60^\circ$ and $h_{\rm d} = 10^8$ cm.

Table 3 Variations of the Source Size R'', the Electron Number Density *N*, and the Total Number Density $N_{\rm total}$ in the MW and THz Emission Regions of the 2003 November 2 Burst.

Time	MW: R''	N (cm^{-3})	$N_{\rm total}$ ($\times 10^{35}$)	THz: R''	N (cm^{-3})	$N_{\rm total}$
17:16:15	25	8.0×10^7	2.6	0.5	8×10^6	1.0×10^{31}
17:17:06	25	1.8×10^8	5.9	0.5	4×10^8	5.2×10^{32}
17:17:30	25	1.6×10^8	5.3	0.5	1.0×10^8	1.3×10^{32}
17:18:00	25	1.6×10^8	5.3	0.5	4×10^7	5.2×10^{31}
17:18:30	25	1.6×10^8	5.3	0.5	3×10^8	3.9×10^{32}
17:19:00	25	1.5×10^8	5.0	0.5	2×10^8	2.6×10^{32}
17:19:30	30	1.3×10^8	6.1	0.45	2×10^8	2.2×10^{32}
17:20:00	30	1.3×10^8	6.1	0.45	1.3×10^8	1.4×10^{32}
17:21:00	32	1.3×10^8	7.0	0.38	7×10^7	5.3×10^{31}

N decreased only a little during the decay phase, which are much smaller than in the THz emission source. In the MW source the total electron number doubled during the rise phase. During the decay phase, $N_{\rm total}$ did not decrease but increased from 5.9×10^{35} at the maximum phase to 7×10^{35}, i.e., it increased by about 20%.

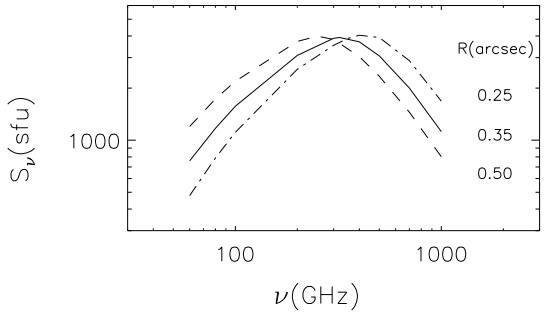

Fig. 5 The effect of the emission source radius R on the modeled GS emission spectrum in the THz range under conditions of a constant total number of electrons, where $\delta = 2.2$, $E_0 = 1.5$ MeV, $B_0 = 5000$ G and $\theta = 10^\circ$.

Here we must point out that in the period from 17:19:30 to 17:21:00 UT of the decay phase, smaller radii ($0.45''$ and $0.38''$) for the THz source are selected to fit these observational spectra. The effect of source size on the THz spectrum can be seen from Figure 5. It shows that the rising rate of flux density at the optically thick part of the THz spectrum increases with decreasing source size and the peak of the modeled spectrum shifts to higher frequency under conditions of a constant total number of electrons. If we still take the same source size ($R = 0.5''$), then the required electron number *N* will largely decrease, which leads to the modeled flux densities of the GS emission at 405 GHz always being lower than values from the observations. Interestingly, we also find that the MW source radius obtained from the spectral fit increased from $25''$ to $32''$ during the decay phase, i.e., the MW source radius increased by 28%.

5 SUMMARY AND CONCLUSIONS

Table 3 shows that the required electron number density *N* in the 2003 November 2 THz emission source increased substantially from 8×10^6 at the rise phase to 4×10^8 cm^{-3} at the maximum phase, i.e., the *N* value increased 50 times from the rise phase to the maximum phase. It means that there would be a very effective electron acceleration mechanism, which can effectively accelerate a huge amount of electrons to a higher energy range of $\sim$1 to 10 MeV in that period. Then *N* began to drop from the maximum value, but it increased once again at 17:18:30 UT and the peak frequency of the fitting spectrum at that time can shift to a higher frequency of 1500 GHz (see Fig. 2). This could result from another effective electron acceleration before $\sim$17:18:30 UT. At 17:21:00 UT it decreased to 7×10^7 cm^{-3}, i.e., decreased about five times from the maximum phase to the decay phase. However, the variation in amplitude of *N* in the MW source only reached about one time during this burst, which is much smaller than that in the THz emission source. During the decay phase, the total electron number $N_{\rm total}$ decreased by an order of magnitude in the THz source, while the value of $N_{\rm total}$ in the

MW source did not decrease but increased from 5.9×10^{35} to 7×10^{35} , i.e., it increased by about 20%.

The dramatic variation of electron number density in the THz emission source could result from the effective electron acceleration at the rise phase and strong electron energy loss at the decay phase. However in the MW source, $N_{\rm total}$ did not decrease but increased by about 20% during the decay phase. There could be many more electrons that decayed from the higher energies which resulted in variation in amplitude of electron number density in the MW source being much smaller than that in the THz source.

It is found that the THz source radius obtained from numerical fits decreased from $0.5''$ to $0.45''$ and even to $0.38''$ during the decay phase, i.e., it decreased by about 24%, but the MW one increased by 28% during the decay phase. Similar variation in source size can also be seen from the study of the 2003 November 4 event (Zhou et al. 2011). This variation in the source size is perhaps a rather interesting result. It would result from variation in the trap height of the energetic electrons, variation in the magnetic field topology, or others.

In the paper we investigate the novel rising THz burst that occurred in super-AR NOAA 10486 on 2003 November 2. Our studies show that it is a steeply rising and very giant THz event. The average rising rate of the flux density reaches 235 sfu $\rm GHz^{-1}$ ($\alpha = 4.8$) for the THz burst. The steeply rising THz spectrum can be produced by energetic electrons with a low-energy cutoff of $\sim$1 MeV and number density of $\sim 10^6$–10^8 $\rm cm^{-3}$ in a compact source ($\sim 0.5''$ in radius) with strong local magnetic fields varying from 4590 to 780 G (2690 G in mean value) via the GS emission in the case of a dipole magnetic field. The average magnetic field strength of 2690 G is much lower than that (4500 G) obtained under the assumption of a uniform magnetic field (see Silva et al. 2007). The photospheric magnetic field of 5000 G would be possible in an observation of a compact source. Unfortunately, because this active region, AR 10486, was close to the limb on November 2, there is no accurate measurement of the photospheric magnetic field. However a magnetic field of 4200 G was measured for AR 10484 (Mt Wilson sunspot group 31909) on 2003 October 22. Since AR 10486 was more active than AR 10484, in fact producing the largest flare on record two days later on November 4, it probably had a very high magnetic field at the time of the November 2 flare, even higher than 4200 G. Notably, Livingston et al. (2006) report that 0.2% of almost 32 000 active regions studied have sunspots with magnetic fields larger than 4000 G, even as high as 6100 G, the highest magnetic field ever measured (see Silva et al. 2007). The associated MW spectral components can be produced by energetic electrons with a 10 keV low-energy cutoff and a mean local magnetic field strength in an extended source with a radius of $25''$–$32''$.

It is found from the numerical simulations of the temporal evolution of spectra that the variation in amplitudes of electron number density and total electron number are much larger in the THz emission source than in the MW source during the burst. In addition, the THz source radius decreased by about 24%, but the MW one increased by 28% during the decay phase. These interesting results would be significant because they can provide important information about the ultrarelativistic electron acceleration, trap, energy loss, and possible evolution in the magnetic field topology at different levels in the burst source region or others. However, we must note that the required source radius is usually much smaller based on the GS emission calculations. Further progress in understanding the physics of THz emission requires observations with a more complete spectral coverage and higher spatial resolution at the THz range.

Acknowledgements The authors thank Dr. V. F. Melnikov for fruitful discussions. This study is supported by the National Natural Science Foundation of China (Grant No. 11333009) and the National Basic Research Program of China (973 program, 2014CB744200).

References

Chertok, I. M., Fomichev, V. V., Gorgutsa, R. V., et al. 1995, Sol. Phys., 160, 181
Croom, D. L. 1973, NASA Special Publication, 342, 114
Gary, D. E. 1985, ApJ, 297, 799
Huang, G., Zhou, A., Su, Y., & Zhang, J. 2005, New Astron., 10, 219
Kaufmann, P., Correia, E., Costa, J. E. R., Vaz, A. M. Z., & Dennis, B. R. 1985, Nature, 313, 380
Kaufmann, P., Raulin, J.-P., de Castro, C. G. G., et al. 2004, ApJ, 603, L121
Krucker, S., Giménez de Castro, C. G., Hudson, H. S., et al. 2013, A&A Rev., 21, 58
Livingston, W., Harvey, J. W., Malanushenko, O. V., & Webster, L. 2006, Sol. Phys., 239, 41
Lüthi, T., Lüdi, A., & Magun, A. 2004a, A&A, 420, 361
Lüthi, T., Magun, A., & Miller, M. 2004b, A&A, 415, 1123
Ramaty, R., Schwartz, R. A., Enome, S., & Nakajima, H. 1994, ApJ, 436, 941
Silva, A. V. R., Share, G. H., Murphy, R. J., et al. 2007, Sol. Phys., 245, 311
Trottet, G., Raulin, J.-P., Kaufmann, P., et al. 2002, A&A, 381, 694
Wang, H., Gary, D. E., Lim, J., & Schwartz, R. A. 1994, ApJ, 433, 379
Zhou, A.-H., & Karlicky, M. 1994, Sol. Phys., 153, 441
Zhou, A. H., Su, Y. N., & Huang, G. L. 2005, Sol. Phys., 226, 327
Zhou, A. H., Li, J. P., & Wang, X. D. 2008, Sol. Phys., 247, 63
Zhou, A.-H., Wang, R.-C., & Shao, C.-W. 2009, RAA (Research in Astronomy and Astrophysics), 9, 475
Zhou, A. H., Li, J. P., & Wang, X. D. 2011, ApJ, 727, 42